As-bearing new mineral species from Valletta mine, Maira Valley, Piedmont, Italy: II. Braccoite, NaMn2+5[Si5AsO17(OH)](OH), description and crystal structure

Revision 1

As-bearing new mineral species from Valletta mine, Maira Valley, Piedmont, Italy: II. Braccoite, $NaMn^{2+}_5[Si_5AsO_{17}(OH)](OH)$, description and crystal structure

FERNANDO CÁMARA[1,2]*, ERICA BITTARELLO[1,2], MARCO E. CIRIOTTI[3], FABRIZIO NESTOLA[4], FRANCESCO RADICA[5] AND MARCO MARCHESINI[6]

[1]Dipartimento di Scienze della Terra, Università degli Studi di Torino, via Tommaso Valperga Caluso 35, I-10125 Torino, Italy

[2]CrisDi, Interdepartmental Centre for the Research and Development of Crystallography, via Pietro Giuria 7, I-10125, Torino, Italy

[3]Associazione Micromineralogica Italiana, via San Pietro 55, I-10073 Devesi-Cirié, Torino, Italy

[4]Dipartimento di Geoscienze, Università degli Studi di Padova, via Giovanni Gradenigo 6, I-35131 Padova, Italy

[5]Dipartimento di Scienze Geologiche, Università degli Studi Roma Tre, largo San Leonardo Murialdo 1, I-00146 Roma, Italy

[6] EEEP house, UNIR, Basing View, Basingstoke, Hampshire, RG21 4YY, United Kingdom

*correspondent author's e-mail: fernando.camaraartigas@unito.it

ABSTRACT

The new mineral species braccoite, ideally $NaMn^{2+}_5[Si_5AsO_{17}(OH)](OH)$, has been discovered in the Valletta mine dumps, in Maira Valley, Cuneo province, Piedmont, Italy. Its origin is probably related to the reaction between ore minerals and hydrothermal fluids. It occurs as subhedral crystals that occurs in brown-red coloured thin masses, with pale yellow streak and vitreous to resinous luster. Braccoite is associated with tiragalloite, of which new data is provided, as well as gamagarite, hematite, manganberzeliite, palenzonaite, quartz, saneroite, tokyoite, unidentified Mn oxides, organic compounds, and Mn arsenates and silicates under study.

Braccoite is biaxial positive with refractive indices α 1.749(1), β 1.750(1), γ 1.760(1). It is triclinic, space group $P\bar{1}$, with a = 9.7354(4), b = 9.9572(3), c = 9.0657(3) Å, α = 92.691(2)°, β = 117.057(4)°, γ = 105.323(3)°, V = 740.37(4) Å^3 and Z 2. Its calculated density is 3.56 g/cm^3. The ten strongest diffraction lines of the observed X-ray powder diffraction pattern are [d in Å, (I), (hkl)]: 3.055 (69)(2$\bar{2}$1), 3.042 (43)(102), 3.012 (65)(3$\bar{2}$1), 2.985 (55)(2$\bar{3}$1), 2.825 (100)(21$\bar{3}$), 2.708 (92)(220), 2.627 (43)(2$\bar{3}$2), 2.381 (58)(4$\bar{1}$1), 2.226 (25)(214), and 1.680 (43$\bar{3}$)(36). Chemical analyses by WDS electron microprobe gave (wt%): Na_2O 4.06, CaO 0.05, MnO 41.76, MgO 0.96, Al_2O_3 0.04, CuO 0.02, SiO_2 39.73, As_2O_5 6.87, V_2O_5 1.43, SO_3 0.01, and F 0.04. H_2O 2.20 was calculated on the basis of 2OH groups p.f.u. Raman spectroscopy confirmed the presence of $(SiO_4)^{4-}$, $(AsO_4)^{3-}$ and OH groups. The empirical formula calculated on the basis of Σ cations-(Na,K) = 11 p.f.u., in agreement to the results of crystal structure, is $Na_{1.06}(Mn^{2+}_{4.46}Mn^{3+}_{0.32}Mg_{0.19}V^{3+}_{0.01}Al_{0.01}Ca_{0.01})[Si_5(As_{0.48}Si_{0.37}V^{5+}_{0.15})O_{17}(OH)](OH_{0.98}F_{0.02})$, the simplified formula is $Na(Mn,Mg,Al,Ca)_5[Si_5(As, V, Si)O_{17}(OH)](OH,F)$.

Single crystal X-ray diffraction allowed us to solve the structure by direct methods and revealed that braccoite is the As-dominant analogue of saneroite. The structure model was refined on the basis of 4389 observed reflections to R_1 3.47 %. Braccoite is named in honor of Dr. Roberto Bracco (b. 1959), a systematic collector with a special interest in manganese minerals. The new mineral was approved by IMA 2013-093.

Keywords: braccoite, saneroite, arseno-silicates, tiragalloite, new mineral species, crystal structure, Raman, Valletta, Piedmont, Italy

INTRODUCTION

This is the second of a series of new mineral descriptions of As–bearing minerals from Valletta mine (Cámara *et al*. 2014). The sample containing braccoite, the As-analogue of saneroite, was collected by one of the authors (MM) in 2012 in the dumps of Valletta mine, Vallone della Valletta, Canosio municipality, Maira Valley, Cuneo province, Piedmont, Italy (44°23'54" N, 7°5'42" E, 2536 m asl).

The name is in honour of Dr. Roberto Bracco (b. 1959), a systematic collector with a special interest in manganese minerals (Barresi *et al.*, 2005; Bracco and Balestra, 2014). He has authored or coauthored several publications on systematic mineralogy, especially devoted to new occurrences in Liguria (Bracco *et al.*, 2006; 2012).

A fragment of the holotype material is deposited in the mineralogical collections of the Museo Regionale di Scienze Naturali di Torino, Sezione di Mineralogia, Petrografia e Geologia, Torino, Italy, catalogue number M/15939.

Braccoite is intergrown with tiragalloite, which is an infrequent mineral. For this reason we provide additionally chemical and Raman spectrum of tiragalloite [$Mn^{2+}_4As^{5+}Si_3O_{12}(OH)$] from Valletta mine.

GEOLOGICAL SETTING AND MINERAL OCCURRENCE

Geological and historical brief information is provided in Cámara *et al*. (2014). The deposit at Valletta mine has never been studied from a genetic point of view and available geological data for the area are of limited detail. Other than the historic texts, there is no mention in the literature of the occurrence of metalliferous mineralization in this locality. Preliminary work carried out during sampling showed that it is a small iron deposit with subordinate manganese, in quartzites with quartz veins that contain a large variety of mineral phases rich in arsenic, vanadium, barium and strontium. The volume of mineralized body is however rather limited in surface.

The rock hosting braccoite is compact, granular, dark red verging on black quartzite. Blocks of this material have been dug and piled up in a small landfill where they are mixed with calcareous rocks also from the excavated material.

Braccoite is strictly associated with tiragalloite, and with gamagarite, hematite, manganberzeliite, palenzonaite, quartz, saneroite, tokyoite, unidentified Mn oxides, organic compounds, and Mn arsenates and silicates under study. These findings make in terms of mineralogical variety the small dump of the old Valletta mine one of the richest Italian deposits of arsenates and silicoarsenates mineral phases, like those of Val Graveglia (Antofilli

et al. 1983; Borgo and Palenzona, 1988; Palenzona, 1991, 1996; Marchesini and Pagano, 2001). Other As-rich minerals found in the rock samples collected in the dump, although not strictly associated with braccoite are: adelite $CaMg(AsO_4)(OH)$, arseniopleite-caryinite series $(Ca,Na)NaMn^{2+}(Mn^{2+},Mg,Fe^{2+})_2(AsO_4)_3$-$(Na,Pb)(Ca,Na)CaMn^{2+}{}_2(AsO_4)_3$, bariopharmacosiderite $Ba_{0.5}Al_4(AsO_4)_3(OH)_4{\cdot}4H_2O$, berzeliite $NaCa_2Mg_2(AsO_4)_3$, grandaite $Sr_2Al(AsO_4)_2(OH)$ (IMA2013-059), and tilasite $CaMg(AsO_4)F$; these are found along with aegirine, albite, azurite, baryte, braunite, calcite, diopside, fluorapatite, ganophyllite, gypsum, ilmenite, hollandite, malachite, magnesio-arfvedsonite, magnesio-riebeckite, magnetite, mimetite, muscovite, neotocite, opal, orthoclase, phlogopite, ranciéite, richterite, rutile, rhodonite, talc, tetrahedrite, titanite and some other unknown phases under investigation.

MINERALOGICAL CHARACTERIZATION

Appearance and physical properties

Braccoite occurs as subhedral equant crystals, few hundred of micrometers accros, with uneven fracture, grouped in thin masses, a few centimeters in size (Fig. 1), on granular red-brown quartzite with reddish-brownish-black K-feldspar and compact quartz. In rare cases the mineral forms rims around the remnants of protolithic quartz clasts. Individual crystals are brown-red coloured and translucent. Braccoite has a pale yellow streak, a vitreous to resinous luster, and does not fluoresce under SW or LW ultraviolet light. Braccoite is optically biaxial positive, with a $2V_{meas}$ = 26(2)º and $2V_{calc}$ = 35º. The measured refractive indices are α = 1.749(1), β = 1.750(1), and γ = 1.760(1) (589 nm). Braccoite is weakly pleochroic with X = brownish yellow, Y = dark yellow, Z = yellow. The mineral is brittle and no cleavage and parting are observed. Hardness and density were not measured due to the small crystal size and because it occurs intimately intergrown with tiragalloite. The calculated density obtained from the empirical formula and unit-cell parameters of the single crystal used for the crystal-structure determination is 3.56 g/cm^3.

Chemical data

Chemical composition of braccoite was determined using a Cameca SX–50 electron microprobe (WDS mode) at the Department of Geosciences (Università di Padova) on a thin section obtained from the holotype close to the place where the crystal used for the diffraction study was extracted. Major and minor elements were determined at 20 kV accelerating voltage and 20 nA beam current (beam size 2 μm), with 40 to 20 s counting time on both peak

and background. X–ray counts were converted to oxide wt% using the PAP correction program supplied by Cameca (Pouchou and Pichoir, 1984; 1985). The crystals studied in the thin section (Fig. 2) were found to be homogeneous. Fe, Sb and Pb were analysed for but were below detection limits. H_2O was calculated on the basis of 2OH groups p.f.u. (Nagashima and Armbruster, 2010a). The average of 5 analyses are given in Table 1a. Low totals are related to the difficulty of preparing good thin sections of polymineralic aggregates, but have been also reported for saneroite samples (Nagashima and Armbruster, 2010a).

The empirical formula, calculated on the basis of 19 O a.p.f.u. and considering 2(OH) is, within rounding errors, $Na_{1.06}(Mn^{2+}_{4.46}Mn^{3+}_{0.32}Mg_{0.19}Al_{0.01}Ca_{0.01})_{\Sigma 4.99}$ $[(Si_{5.36}As_{0.48}V_{0.15})_{\Sigma 5.99}$ $O_{17}(OH)]$ $(OH_{0.98}F_{0.02})$. Alternatively, the empirical formula, calculated on the basis of Σ cations-(Na,K) = 11, Mn^{2+}/Mn^{3+}ratio calculated in order to obtain [2(OH)-(Na-0.5)] groups p.f.u. [Mn^{3+}/(total Mn) = 0.066] and tetrahedral V^{5+} calculated as 6 – (Si + As), and excess V is assigned to the octahedral sites as V^{3+}, following Nagashima and Armbruster (2010a), within rounding errors, is $Na_{1.06}(Mn^{2+}_{4.46}Mn^{3+}_{0.32}Mg_{0.19}V^{3+}_{0.01}Al_{0.01}Ca_{0.01})_{\Sigma=5.00}$ $[Si_{5.37}As^{5+}_{0.48}V^{5+}_{0.15}O_{17}(OH)]$ $(OH_{0.98}F_{0.01})$. The simplified formula can be written as: $NaMn^{2+}_5[Si_5AsO_{17}(OH)](OH)$, which requires Na_2O 3.78, MnO 43.31, SiO_2 36.68, As_2O_5 14.03, and H_2O 2.20, total 100 wt%. The presence of OH was confirmed by micro-Raman spectroscopy. The mean refractive index *n* of braccoite, the calculated density and the empirical formula yielded a Gladstone-Dale compatibility index (Mandarino 1979, 1981) of 0.020 rated as excellent. Braccoite is unreactive and insoluble in 2 *M* and 10% HCl, and 65% HNO_3.

In Table 1b we show the comparison between the chemical data of tiragalloite $[Mn^{2+}_4As^{5+}Si_3O_{12}(OH)]$ from Valletta mine and tiragalloite from type-locality of Molinello mine (Ne, Val Graveglia, Liguria, Italy) reported by Gramaccioli *et al*. (1980). Considering a stoichiometric H_2O content in order to have one (OH) group per formula unit (p.f.u.), i.e. 1.46 wt % of H_2O, and 13 oxygen atoms p.f.u., the formula corresponding to the average of 3 analyses is $(Mn^{2+}_{3.92}Mg_{0.06}Na_{0.03})_{\Sigma 4.01}(As^{5+}_{0.87}V^{5+}_{0.05}Si^{4+}_{0.09})_{\Sigma 1.01}Si_3O_{12}(OH_{0.96}F_{0.04})$.

Micro-Raman spectroscopy

The Raman spectrum of braccoite (Fig. 3) was obtained at the Dipartimento di Scienze della Terra (Università di Torino) using a micro/macro Jobin Yvon LabRam HRVIS, equipped with a motorized x-y stage and an Olympus microscope. The backscattered Raman signal was collected with 50× objective and the spectrum was obtained for a non-oriented crystal. The 632.8 nm line of an He-Ne laser was used as excitation; laser power (20 mW)

was controlled by means of a series of density filters. The minimum lateral and depth resolution was set to a few μm. The 532 nm line of a Nd laser was also used as excitation; laser power (80 kW) was dosed by means of a series of density filters. An aperture of 200 μm was used to reduce the beam dose. The lateral and depth resolution were about 2 and 5 μm, respectively. The system was calibrated using the 520.6 cm^{-1} Raman band of silicon before each experimental session. Spectra were collected with multiple acquisitions (2 to 6) with single counting times ranging between 20 and 180 s. The spectrum was recorded using the LabSpec 5 program from 200 to 4000 cm^{-1}. Spectra collected with both lasers were equivalent. Spectrum reported in Fig. 3 was collected with the 632.8 nm line of the He-Ne laser.

There is a close match between the braccoite spectrum and that of saneroite from type locality of Molinello mine (Graveglia Valley, Liguria, Italy) in the database RRUFF (R060488) (Downs, 2006). All bands observed between 700 and 1000 cm^{-1} are characteristic of the two groups present in braccoite, SiO_4^{4-} and $AsO_3(OH)^{2-}$ (Myneni *et al.*, 1998a,b; Nakamoto, 1986). The spectrum shows intense bands around 829, 907 and 932 (respect to 823, 909 and 936 cm^{-1} for saneroite R060488 at RRUFF) and weak peaks at 706 and 748 cm^{-1} (700 and 729 cm^{-1} for saneroite R060488 at RRUFF). The intense peak at 1017 cm^{-1} with a weak shoulder at 1040 cm^{-1} may be assigned to the v_1 symmetric stretching mode of the SiO_4 units (Mills *et al.*, 2005) (1011 and 1022 cm^{-1} for saneroite R060488) while the region assigned in the pyroxenes to the stretching modes of the Si-O bonds is present in the braccoite spectrum at 665 cm^{-1} (respect to 660 cm^{-1} for saneroite R060488). Bending modes of O-Si-O are observed at 525 cm^{-1} and 563 cm^{-1} for braccoite, while Raman spectrum of saneroite R060488 shows a single weak band around 523 cm^{-1}. Cation-oxygen vibration modes appear in the low region of the spectrum below 460 cm^{-1}: weak and broad peaks are observed at 226, 261, 291, 360, 390 and 451 cm^{-1} (respect to 228, 281, 343, 376, 436 cm^{-1} for saneroite R060488). The Raman spectrum of braccoite shows a broad envelope of overlapping bands centered upon 3361 and 3507 cm^{-1}, which are characteristic of OH stretching modes, in accordance with the presence of hydroxyl groups in the structure (spectrum of saneroite R060488 was collected only for < 1200 cm^{-1}).

Tiragalloite is intergrown with braccoite in rocks from Valletta mine. There is no available Raman spectrum for tiragalloite and therefore we collected spectra also for this mineral phase (Fig. 4). The spectrum shows a strong absorption centered at 869 cm^{-1} with three shoulders at 803, 836 and 902 cm^{-1}, two intense peaks at 661 and 647 cm^{-1} and weaker peaks at 960, 975 cm^{-1} and a broad band at ~ 1004 cm^{-1}. As for braccoite and saneroite, the

frequency separations between the bands due to the asymmetric and the symmetric stretches of the anionic groups $(SiO_4)^{4-}$ and $(AsO_4)^{3-}$, present tiragalloite vary strongly from one structure to another, and cannot be assigned with conviction (Hawthorne *et al*., 2013). Bands with frequencies between 250 and 600 cm^{-1} correspond to $(SiO_4)^{4-}$ and $(AsO_4)^{3-}$ vibrations (286, 320, 364, 398, 481, 508 and 549 cm^{-1}), while weak and broad bands lower than 250 cm^{-1} correspond to lattice modes (153, 181 and 218 cm^{-1}). In the region between 1200 and 3000 cm^{-1} the spectrum displays a considerable amount of noise (a broad envelope of overlapping bands centered upon 1635, 1702 and 1799 cm^{-1}) and this is a result of the low intensity of the bands. In accordance with the presence of hydroxyl groups in the structure a wide and weak band at ~3100 cm^{-1}. Based on the Libowitzky (1999) correlation, the band at ~ 3100 cm^{-1} can be possibly assigned to the O11–H11…O1 bond present in tiragalloite (O11…O1 = 2.725 Å corresponding to 3257 cm^{-1}, using crystal data provided by Nagashima and Armbruster 2010b).

X–ray diffraction

The powder X–ray diffraction pattern of braccoite was obtained at CrisDi (Interdepartmental Centre for the Research and Development of Crystallography, Torino, Italy) using an Oxford Gemini R Ultra diffractometer equipped with a CCD area detector, with graphite-monochromatized Mo*K*α radiation. Indexing of the reflections was based on a calculated powder pattern obtained from the structural model, using the software LAZY PULVERIX (Yvon *et al.*, 1977). Experimental and calculated data are reported in Table 2. The unit–cell parameters refined from the powder data with the software GSAS (Larson and Von Dreele, 1994) are a = 9.756(6), b = 9.961(7), c = 9.087(7) Å, α = 92.23(5)°, β = 117.27(5)°, γ = 105.21(4)°, V = 742.2(9) $Å^3$.

Single-crystal X–ray diffraction data were collected using an Oxford Gemini R Ultra diffractometer equipped with a CCD area detector at CrisDi with graphite-monochromatized Mo*K*α radiation (λ = 0.71073 Å). A crystal fragment showing sharp optical extinction behaviour was used for collecting intensity data. No crystal twinning was observed. Crystal data and experimental details are reported in Table 3. The intensities of 7946 reflections with $-13 < h < 14$, $-14 < k < 14$, $-13 < l < 13$ were collected to 64.4° 2θ using 1° frame and an integration time of 20 s. Data were integrated and corrected for Lorentz and polarization background effects, using the package CrysAlisPro, Agilent Technologies, Version 1.171.36.20 (release 27-06-2012 CrysAlis171.36.24). Data were corrected for empirical absorption using spherical harmonics, implemented in the SCALE3 ABSPACK scaling

algorithm. Refinement of the unit-cell parameters was based on 4389 measured reflections with $I > 10\sigma(I)$. At room temperature, the unit-cell parameters are *a* 9.7354(4), *b* 9.9572(3), *c* 9.0657(3) Å, α 92.691(2)°, β 117.057(4)°, γ 105.323(3)°, *V* 740.37(4) Å^3, space group $P\bar{1}$ and *Z* 2. The *a*:*b*:*c* ratio is 0.978:1:0.910. A total of 4911 independent reflections were collected and the structure was solved and refined using the SHELX set of programs (Sheldrick, 2008).

DESCRIPTION OF THE STRUCTURE

Structure model

The crystal structure of braccoite (Figure 5) is topologically identical to that of the hydropyroxenoid saneroite: a single isolated chain of SiO_4 tetrahedra with a five repeat plus an appendix of a sixth tetrahedron where $Si_{1-x}As_x$ substitution occurs ($Si_{1-x}V^{5+}{}_x$ in saneroite). which repeats laterally by a centre of symmetry forming a layer of tetrahedra parallel (1$\bar{1}$1). Five octahedral sites occupied by Mn (mostly Mn^{2+}, with some Mn^{3+}) form a band which runs parallel to two single chains of tetrahedra attached up and down. Laterally the bands are separated by channels occupied partially by two independent Na sites, one completely occupied and another with partial occupation. The structure of braccoite was therefore refined starting from the atom coordinates of saneroite excluding *H* sites (Nagashima and Armbruster, 2010a). Nomenclature of sites follows therefore those of the aforementioned authors. Scattering curves for neutral and ionized atoms were taken from International Tables for Crystallography (Wilson, 1992). Site-scattering values were refined for the cation sites using two scattering curves contributing proportionally and constrained sum to full occupancy: Mn^{2+} and Mg were used for the sites *Mn*(1-5); Si^{4+} full occupancy was fixed at the *T*(1-5) sites, while Si^{4+} and As were used at *T*(6) site; Na^+ was used for the *Na*(1) and *Na*(2) sites, although the occupancy was held fixed at *Na*(1) and refined at *Na*(2). After converging, the positions of two H atoms [*H*(7) and *H*(19) sites] were located in difference Fourier maps and added to the model; atom coordinates of *H* sites were refined and isotropic thermal parameters were constrained to be 1.2 times the isotropic equivalent of the oxygen atom of the hydroxyl group assuming a riding motion model, while a soft constraint of 0.98 Å (Franks, 1973) was applied to the *H*(19)–O(19) distance. Structure refinement converged to $R_1 = 0.0347$ for 4389 reflections with $F_o > 4\sigma(F_o)$ and 0.0413 for all 4911 data. Tables 4, 5 and 6 report atomic coordinates, the displacement parameters and selected bond distances and angles respectively for braccoite. Bond valence calculations using the parameters of Brown (1981) are reported in Table 7. (CIF[1] and structure factor list files are available on deposit).

Site occupancies

Cation sites

There are 13 cation sites in the braccoite structure: 6 sites are 4-coordinated, 5 sites are 6-coordinated, and 2 are 8-coordinated. One out of the six 4-coordinated sites, the *T*(6) site, has a higher mean atomic number [24.17(6) electrons per site (e.p.s.) versus 14 e.p.s. for the other 5 sites, Table 4], and <T-O> is larger than that the other 5 sites (1.675 Å vs. a mean of 1.624 Å for the other 5 sites, Table 6). Chemical analyses report the presence of both V^{5+} and As^{5+} that can order in a site with tetrahedral coordination. The refined site scattering is > 23 e.p.s. and therefore implies dominance of As in presence of sufficient amount of Si. The latter is confirmed by EMP analyses (Table 1a). In presence of concomitant Si-V-As solid solution in a cation site with tetrahedral coordination, the size of the tetrahedron is not sufficient to provide the actual dominance of As^{5+} versus V^{5+} because they have very similar ionic radii (0.335 and 0.355 Å, respectively, Shannon 1976). While distances observed in the studied crystal (Table 6) are compatible with a Si–V substitution (values of 1.68-169 Å are usually found for saneroite, Nagashima and Armbruster, 2010a, and ca. 1.70 Å for medaite, Nagashima and Armbruster, 2010b), It is worth noting that besides the chemical strain due to a three component solid solution, the *T*(6) is not the most distorted 4-coordinated site in the structure: the *T*(5) shows the highest angle variance [σ^2 41.72, computed according to Robinson *et al*. 1971, Table 6] as similarly observed in saneroite (σ^2 = 40.00, Basso and Della Giusta, 1980).

Regarding the 5 sites 6-coordinated, all are Mn^{2+} dominant. However, site *Mn*(3) is significantly smaller (2.183 Å versus 2.20-2.25 Å, Table 6). This can be interpreted as ordering of a lighter and smaller Mg cation, which is present in the chemical analyses. Yet ordering all the Mg at the *Mn*(3) site would require a site scattering value lighter than that observed. On the other hand, a small quantity of Mn^{3+} has been inferred in the chemical formula (see Chemical data section) in order to achieve charge balance assuming full occupancy of H at the *H*(7) and *H*(19) sites. In addition, Nagashima and Armbruster (2010a) confirmed the presence of a limited quantity of Mn^{3+} in saneroite form Molinello (Val Graveglia, Italy) by using the ratio of the X-ray intensities of the Mn*L*β and Mn*L*α lines after the method of Albee and Chodos (1970) and Kimura and Akasaka (1999). Therefore, we assumed also for braccoite a limited amount of Mn^{3+} (0.066 Mn^{3+}/Mn_{total}). Incidentally, other Mn^{3+} phases have been found at the Valletta mine (es. grandaite, Cámara *et al*., 2014) and all the iron–bearing phases have just Fe^{3+}. Because there is not a high bond valence contribution

to the *Mn*(3) site (Table 7) it is probable that Mn^{3+} distributes also in the other two smaller sites, *Mn*(2) and *Mn*(4). In the structure of braccoite there is also one octahedron that is slightly larger than the others, the *Mn*(1) site. Apparently, it should host the very small amount of Ca in the analyses, although that amount is not enough to justify the observed size enlargement. However, Ca could also distribute at the *Na*(1) or *Na*(2) sites. The *Mn*(1) site is also the more distorted (σ^2 = 170.51, compared to values ranging between 55.18 and 86.77, Table 6). This is possibly due to the fact that the oxygen at O(16) acts as bond donor to the proton at *H*(19) and that it is the only octahedron that shares an edge with a tetrahedron, the *T*(5) site, which is also the most distorted tetrahedron. The O(5)-O(14) edge involves two anion sites with among the highest and the lowest bond valence contribution, respectively (Table 7) and is also the shortest. Hence there is a possible charge-shielding mechanism operated by the electronic clouds of both oxygen atoms.

The 8-coordinated sites host Na atoms. The *Na*(1) site has full occupancy and bond distances compatible with 1 a.p.f.u. of Na (Table 8), while the *Na*(2) site shows a refined site scattering which indicates approx. half occupancy of Na (Table 4). This site shares four edges with four Si tetrahedra and two edges with two Mn octahedra [*Mn*(2) and *Mn*(5)]. This is probably impeding the full occupancy of this site and produces a rather distorted bonding environment.

Taking into consideration the observed site scattering values and those obtained from EMP analyses, the agreement for all cations sites is within 2% relative error, with slightly lighter values from diffraction data than obtained from chemical analyses (230.8 electrons per formula unit, e.p.f.u., versus 233.9 e.p.f.u., respectively). Site-distribution according to the structure refinement (site scattering and bond distances) and electron microprobe data results give full occupancy of Si at the *T*(1-5) sites, *T*6 ($As^{5+}_{0.48}Si_{0.37}V^{5+}_{0.15}$), *Mn*1 ($Mn^{2+}_{0.98}Mg_{0.01}Ca_{0.01}$), *Mn*2 ($Mn^{2+}_{0.87}Mn^{3+}_{0.07}Mg_{0.06}$), *Mn*3 ($Mn^{2+}_{0.66}Mn^{3+}_{0.22}V^{3+}_{0.01}Al_{0.01}Mg_{0.10}$), *Mn*4 ($Mn^{2+}_{0.96}Mn^{3+}_{0.03}Mg_{0.01}$), *Mn*5 ($Mn^{2+}_{0.99}Mg_{0.01}$), *Na*1 ($Na_{1.00}$), *Na*2 ($Na_{0.56}$), with an overall positive charge of 36.53. Table 8 reports the agreement between observed values and those calculated from chemical composition after site assignment.

Anion sites

There are 19 anion sites in the structure of braccoite, 10 are 3-coordinated and the rest are 4-coordinated (Table 7). There are three anion sites with a bond valence incidence significantly higher than 2 v.u.: O(4), O(5) and O(6). The same atoms show also high bond

valence incidence for saneroite (Basso and Della Giusta, 1980; Nagashima and Armbruster 2010a), in particular O(4), which is 3-coordinated; at the O(4) site, the contribution from *T*(3) and *T*(4) is already 2.011 v.u. and therefore the contribution from the *Na*(2) site (0.134 v.u., Table 7) oversaturates this anion site. This is in fact a strong another restriction for a full occupancy of the *Na*(2) site (see above).

Two anion sites are actually 3-coordinated [O(11) and O(16)] but act as donor of two respective hydrogen bonds at O(7) and O(19). Chemical analyses show a very limited amount of fluorine. While it is not possible to assess in which site the fluorine orders, it is highly probable that it orders at the O(19) site: this site receives a bond valence contribution of 1.091 v.u. (Table 7) and therefore hosts an (OH) group, which belongs to three octahedra of two *Mn*(3) and one *Mn*(2) site. The Raman spectrum at Figure 3 shows a broad envelope of overlapping bands centered upon 3361 and 3507 cm^{-1}, which are reflecting the two essential next neighbor configurations: $Mn^{2+}Mn^{2+}Mn^{2+}$ and $Mn^{3+}Mn^{3+}Mn^{2+}$, while other configurations are also possible, i.e. $MgMgMn^{2+}$, $Mn^{3+}Mn^{3+}Mn^{3+}$ or even MgMgMg, yielding in the overall a broad band. Hydrogen bonding is also present at the O(7) anion site. However, in this case, a short distance with another oxygen atom at the O(11) anion site (2.48 Å) along with a similar bond valence contribution, of 1.531 for O(7) and 1.524 v.u. for O(11), is probably responsible for a very strong hydrogen bond (see later).

Hydrogen bonding

Strong hydrogen bonding is present in the braccoite structure as it was observed in saneroite. A close inspection of Table 7 shows that there are four oxygen sites with bond valence incidence < 1.8 v.u: O(7), O(11), O(16) and O(19). There is one very short acceptor-donor distance corresponding to a very strong hydrogen bond [O(7)…O(11) = 2.48 Å, Table 6], and another longer distance corresponding to a medium strength hydrogen bond (O(19)…O(16) = 2.855 Å, Table 6). Using the relation $\nu(cm^{-1}) = 3592-304\times10^{9}\cdot\exp(-d(O\ldots O)/0.1321)$ (Libowitzky, 1999), we should expect bands at 1456 and 3467 cm^{-1}. While frequencies at ca. 3500 cm^{-1} are observed in the Raman spectrum of braccoite (Fig. 3) the expected band around 1400 cm^{-1} is not visible in the spectrum. The positions of two hydrogen atoms were observed in the Fourier-difference maps at convergence and were added to the model. In particular, the position observed for the *H*(7) atom shows a bond with oxygen at the O(7) anion site with a short *H*(7)…O(11) distance of 1.62(4) Å. The position of the corresponding hydrogen atom in saneroite was not detected by Basso and Della Giusta (1980) but was found with very similar atom coordinates by

Nagashima and Armbruster (2010a) (x = 0.937(5) y = 0.493(4) z = 0.820(5) for braccoite and x = 0.940(3) y = 0.506(3) z = 0.815(4) for saneroite specimen 1 of Nagashima and Armbruster, 2010a, Table 3), and in fact a band at ca. 1400 cm^{-1} was observed in the FT-IR spectrum collected on saneroite from Molinello by Brugger *et al*. (2006). The fact that both O(7) and O(11) show an equivalent bond valence contribution (Table 7), suggests a plausible disordered environment for this proton. Such a situation, with a disordered position for H, has been already observed in another related pyroxenoid structure, serandite ($NaMn_2[Si_3O_8(OH)]$), which shows a O…O distance of 2.464–2.468 Å (Jacobsen *et al*., 2000) and for which the IR O–H stretching mode was found at 1386 cm^{-1} (Hammer *et al*., 1998). Another topologically related structure is scheuchzerite ($NaMn^{2+}_9[Si_9V^{5+}O_{28}(OH)](OH)_3$; Brugger *et al*., 2006), which has also a very strong hydrogen bond among O(26) and O(29) anion sites, distant by 2.35 Å (Brugger *et al*., 2006). In this case a band is observed at 1466 cm^{-1} in the FTIR spectrum, which can correspond to the strong hydrogen bond. It should be also taken into account that the *H*(7) site is at a distance of 2.09(5) Å of the *Na*(2) site, which is not far of the Na-H distance in NaH (1.913 Å; Chen *et al*., 2005) and this surely stresses the bonding environment of the proton at ca. half of the *H*(7) sites.

RELATED MINERALS

Braccoite, $NaMn^{2+}_5[Si_5AsO_{17}(OH)](OH)$, is the As–dominant analogue of saneroite, $NaMn^{2+}_5[Si_5V^{5+}O_{17}(OH)](OH)$ (Basso and Della Giusta, 1980; Lucchetti *et al*., 1981; Nagashima and Armbruster, 2010a). For the dominant cation in *T*6 site Nagashima and Armbruster (2010) proposed to add a suffix, i.e. "saneroite-(V)", "saneroite-(Si)" and "saneroite-(As)". In the recent IMA guidelines, Hatert *et al*. (2013) allow the use of any another name confirming that "mineral names are chosen by the authors of new mineral species, according to functional guidelines established by the Nickel & Grice (1998)" . A new name was chosen to avoid suffixing saneroite so as to preserve *in toto* this "well-established name" and also to meet with the preferences of the collectors community.

Braccoite has also structural similarity with scheuchzerite, $NaMn^{2+}_9[Si_9V^{5+}O_{28}(OH)](OH)_3$ (Brugger *et al*., 2006; Palenzona *et al*., 2006; Roth, 2007): while saneroite/braccoite have a silicate single-chain with five tetrahedra in the repeating unit – with an additional tetrahedron branching sideways (Fig. 5) – scheuchzerite has a chain that consists of the branched saneroite chain with additional attached silicate tetrahedra, configuring "loops" (Brugger *et al*., 2006). These "loops" are also present in a new Na-Mn borosilicate, steedite $NaMn^{2+}_2[Si_3BO_9(OH)](OH)$ (IMA2013-052), which crystal structure

closely resembles those of the sérandite-pectolite pyroxenoids and it is also broadly similar to the crystal structure of scheuchzerite (Haring and McDonald, 2014).

Braccoite is the first As member of the saneroite family and in Table 9 we have reported a comparison of the properties of the members. In the Strunz System (Strunz and Nickel, 2001) braccoite fits in subdivision 9.D.K, inosilicates with 5-periodic single chains. Its equivalent synthetic compound is not known.

ACKNOWLEDGMENTS

The authors are indebted to Bruno Lombardo, who passed away some days after the identification of this new species, for his assessment support in field work at the Valletta. Mariko Nagashima, Gerald Giester, Peter Leverett and associate editor Stuart Mills are thanked for their constructive comments on the manuscript. FC and EB thank MIUR and AMI for the co-funding of a research contract for EB for the year 2013. Raul Carampin (CNR-IGG, Padova, Italy) is thanked for his support on the WDS analysis.

REFERENCES

Albee, A. and Chodos, A.A. (1970) Semiquantitative electron microprobe determination of Fe^{2+}/Fe^{3+} and Mn^{2+}/Mn^{3+} in oxides and silicates and its application to petrologic problems. *American Mineralogist*, **55**, 491–501.

Albrecht, J. (1990) An As-rich manganiferous mineral assemblage from the Ködnitz Valley (Eastern Alps, Austria): geology, mineralogy, genetic considerations, and implications for metamorphic Mn deposits. *Neues Jahrbuch für Mineralogie, Monatshefte*, 363−375.

Antofilli, M., Borgo, E., and Palenzona, A. (1983) *I nostri minerali. Geologia e mineralogia in Liguria*, 296 p. SAGEP Editrice, Genova (in Italian). Barresi, A.A., Kolitsch, U., Ciriotti, M.E., Ambrino, P., Bracco, R., and Bonacina, E. (2005) La miniera di manganese di Varenche (Aosta, Italia nord-occidentale): ardennite, arseniopleite, manganberzeliite, pirofanite, sarkinite, thortveitite, nuovo As−Sc−analogo della metavariscite e altre specie. *Micro*, **3**, 81−122 (in Italian).

Basso, R., and Della Giusta, A. (1980) The crystal structure of a new manganese silicate. *Neues Jahrbuch für Mineralogie, Abhandlungen*, **138**, 333−342.

Bracco, R. and Balestra, C. (2014) La miniera di Monte Nero, Rocchetta Vara, La Spezia, Liguria: minerali classici e novità. *Micro*, **12**, 2−28 (in Italian).

Bracco, R., Balestra, C., Castellaro, F., Mills, S.J., Ma, C., Callegari, A.M., Boiocchi, M., Bersani, D., Cadoni, M., and Ciriotti, M.E. (2012) Nuovi minerali di Terre Rare da Costa Balzi Rossi, Magliolo (SV), Liguria. *Micro*, **10**, 66−77 (in Italian).

Bracco, R., Callegari, A., Boiocchi, M., Balestra, C., Armellino, G., and Ciriotti, M.E. (2006) Costa Balzi Rossi (Magliolo, Val Maremola, Savona, Liguria): una nuova località per minerali di Terre Rare e scandio. *Micro*, **4**, 161−178 (in Italian).

Borgo, E. and Palenzona, A. (1988) *I nostri minerali. Geologia e mineralogia in Liguria. Aggiornamento* 1988, 48 p. SAGEP Editrice, Genova (in Italian).

Brown, I.D. (1981) The bond-valence method: an empirical approach to chemical structure and bonding. Pp. 1–30. *Structure and Bonding in Crystals* II, (M. O'Keeffe and A. Navrotsky, editors), Academic Press, New York.

Brugger, J., Krivovichev, S., Meisser, N., Ansermet, S., and Armbruster, T. (2006) Scheuchzerite, $Na(Mn,Mg)_9[VSi_9O_{28}(OH)](OH)_3$, a new single-chain silicate. *American Mineralogist*, **91**, 937−943.

Cámara, F., Ciriotti, M.E., Bittarello, E., Nestola, F., Massimi, F., Radica, F., Costa, E., Benna, P., and Piccoli, G.C. (2014) As−bearing new mineral species from Valletta mine, Maira Valley, Piedmont, Italy: I. Grandaite, $Sr_2Al(AsO_4)_2(OH)$, description and crystal structure. *Mineralogical Magazine*, (in press).

Chen Y.L., Huang, C.H. and Hu, W.P. (2005) Theoretical study of the small clusters of LiH, NaH, BeH_2, and MgH_2. *The Journal of Physical Chemistry* A, **109**, 9627−9636.

Downs, R.T. (2006) The RRUFF Project: an integrated study of the chemistry, crystallography, Raman and infrared spectroscopy of minerals. Program and Abstracts of the 19th General Meeting of the International Mineralogical Association in Kobe, Japan. O03-13

Franks, F., ed. (1973): Water: a comprehensive treatise, Vol. 2. Plenum, New York, 684 p.

Gramaccioli C. M., Griffin W.L., Mottana A. (1980) Tiragalloite, $Mn_4[AsSi_3O_{12}(OH)]$, a new mineral and the first example of arsenatotrisilicate. *American Mineralogist*, **65**, 947−952.

Hammer, V.M.F., Libowitzky, E., Rossman, G.R. (1998) Single crystal IR spectroscopy of very strong hydrogen bonds in pectolite, $NaCa_2[Si_3O_8(OH)]$, and serandite, $NaMn_2[Si_3O_8(OH)]$. *American Mineralogist*, **83**, 569–576.

Haring, M.M.M., McDonald A.M. (2014) Steedeite, $NaMn_2[Si_3BO_9](OH)_2$: characterization, crystal-structure determination, and origin. *Canadian Mineralogist*, **52**, 47-60.

Hatert, F., Mills, S.J., Pasero, M., Williams, P.A. (2013) CNMNC guidelines for the use of suffixes and prefixes in mineral nomenclature, and for the preservation of historical names. *European Journal of Mineralogy*, **25**, 113–115.

Hawthorne F.C., Abdu Y.A., Ball N.A, Pinch W.W. (2013) Carlfrancisite: $Mn^{2+}_3(Mn^{2+},Mg,Fe^{3+},Al)_{42}(As^{3+}O_3)_2(As^{5+}O_4)_4[(Si,As^{5+})O_4]_6[(As^{5+},Si)O_4]_2(OH)_{42}$, a new arseno-silicate mineral from the Kombat mine, Otavi Valley, Namibia. *American Mineralogist*, **98**, 1693−1696.

Jacobsen, S.D., Smyth, J.R., Swope, R.J., Sheldon, R.I. (2000) Two proton positions in the very strong hydrogen bond of serandite, $NaMn_2[Si_3O_8(OH)]$. *American Mineralogist*, **85**, 745–752.

Kimura, Y. and Akasaka, M. (1999) Estimation of Fe^{2+}/Fe^{3+} and Mn^{2+}/Mn^{3+} ratios by electron probe micro analyzer. *Journal of the Mineralogical Society of Japan*, **28**, 159–166 (in Japanese with English abstract).

Larson, A.C., and Von Dreele, R.B. (1994) General Structure Analysis System (GSAS). Los Alamos National Laboratory Report LAUR, 86−748.

Libowitzky, E. (1999) Correlation of OH stretching frequencies and O–H…O hydrogen bond lengths in minerals. *Monatshefte für Chemie*, **130**, 1047–1059.

Lucchetti, G., Penco, A.M., and Rinaldi, R. (1981) Saneroite, a new natural hydrated Mn-silicate. *Neues Jahrbuch für Mineralogie, Monatshefte*, 161−168.Mandarino, J.A. (1979) The Gladstone-Dale relationship. Part III. Some general applications. *The Canadian Mineralogist*, **17**, 71–76.

Mandarino, J.A. (1981) The Gladstone-Dale relationship. Part IV. The compatibility concept and its application. *The Canadian Mineralogist*, **19**, 441–450.

Marchesini, M. and Pagano, R. (2001) The Val Graveglia Manganese District, Liguria, Italy. *Mineralogical Record*, **32**, 349−379.

Mills, S.J., Frost, R.L., Kloprogge, J.T., and Weier, M.L. (2005) Raman spectroscopy of the mineral rhodonite. *Spectrochimica Acta*, **62**, 171−175.

Momma, K. and Izumi, F. (2011) "VESTA 3 for three-dimensional visualization of crystal, volumetric and morphology data. Journal of Applied Crystallography, **44**, 1272−1276.

Myneni, S.C.B., Traina, S.J., Waychunas, G.A., and Logan, T.J. (1998a) Experimental and theoretical vibrational spectroscopic evaluation of arsenate coordination in aqueous solutions and solids. *Geochimica et Cosmochimica Acta*, **62**, 3285−3300.

493 Myneni, S.C.B., Traina, S.J., Waychunas, G.A., and Logan, T.J. (1998b) Vibrational
494 spectroscopy of functional group chemistry and arsenate coordination in ettringite.
495 *Geochimica et Cosmochimica Acta*, **62**, 3499−3514.
496 Nakamoto, K. (1986) Infrared and Raman Spectra of Inorganic and Coordination Compounds,
497 419 pp. Wiley, New York.
498 Nagashima, M., and Armbruster, T. (2010a) Saneroite: chemical and structural variations of
499 manganese pyroxenoids with hydrogen bonding in the silicate chain. *European Journal*
500 *of Mineralogy*, **22**, 393−402.
501 Nagashima, M., and Armbruster, T. (2010b) Ardennite, tiragalloite and medaite: structural
502 control of $(As^{5+},V^{5+},Si^{4+})O_4$ tetrahedra in silicates. *Mineralogical Magazine*, **74**, 55−71.
503 Palenzona, A. (1991) *I nostri minerali. Geologia e mineralogia in Liguria. Aggiornamento*
504 1990, p. 48. Amici Mineralogisti Fiorentini, Associazione Piemontese Mineralogia
505 Paleontologia & Mostra Torinese Minerali, Centro Mineralogico Varesino, Gruppo
506 Mineralogico “A. Negro” Coop Liguria (GE), Gruppo Mineralogico Lombardo, Gruppo
507 Mineralogico Paleontologico “3M” Ferraia (Savona), (in Italian).
508 Palenzona, A. (1996) *I nostri minerali. Geologia e mineralogia in Liguria, Aggiornamento*
509 1995. Rivista Mineralogica Italiana, 2, 149–172 (in Italian).
510 Palenzona, A., Martinelli, A., Bracco, R., and Balestra, C. (2006) IMA 2004-044
511 (scheuchzerite) alla miniera di Gambatesa. *Prie*, **2**, 11−12 (in Italian)
512 Pouchou, J.L., and Pichoir, F. (1984) A new model for quantitative analysis: Part I.
513 Application to the analysis of homogeneous samples. *La Recherche Aerospatiale*, **3**,
514 13−38.
515 Pouchou, J.L., and Pichoir, F. (1985) `PAP' φ(ρZ) procedure for improved quantitative
516 microanalysis. In J.T. Armstrong, Ed., *Microbeam Analysis*, p. 104−106. San Francisco
517 Press, San Francisco, California.
518 Robinson, K., Gibbs, G.V., and Ribbe, P.H. (1971) Quadratic elongation: a quantitative
519 measure of distortion in coordination polyhedra. *Science*, **172**, 567−570.
520 Roth, P. (2007) Scheuchzerite. In Minerals First Discovered in Switzerland and Minerals
521 Named after Swiss Individuals. Kristallografik Verlag, Achberg, p.130−131.
522 Shannon, R.D. (1976) Revised effective ionic radii and systematic studies of interatomie
523 distances in halides and chaleogenides. *Acta Crystalographica*, **32**, 751−767.
524 Strunz, H., and Nickel, E.H. (2001) Strunz Mineralogical Tables. Chemical Structural Mineral
525 Classification System. 9th Ed., 870 pp. Schweizerbart, Stuttgart.
526 Sheldrick, G.M. (2008) A short history of SHELX. *Acta Crystallographica*, **A64**, 112–122.

Wilson, A.J.C. (editor) (1992) *International Tables for Crystallography. Volume C: Mathematical, physical and chemical tables*. Kluwer Academic Publishers, Dordrecht, The Netherlands.

Yvon, K., Jeitschko, W., and Parthé, E. (1977) LAZY PULVERIX, a computer program, for calculating X-ray and neutron diffraction powder patterns. *Journal of Applied Crystallography*, **10**, 73−74.

TABLES

Table 1a.

	Wt.%	Range	SD	Probe standard (line)
Na_2O	4.06	3.72-4.22	0.20	albite Amelia (Na*K*α)
CaO	0.05	0.03-0.06	0.01	diopside (Ca*K*α)
MgO	0.96	0.90-1.01	0.05	synthetic periclase (Mg*K*α)
MnO	41.76	40.94-42.46	0.41	$MnTiO_3$ (Mn*K*α)
Mn_2O_3***	3.07	2.55-3.87	0.53	
Al_2O_3	0.04	0.01-0.12	0.04	corundum (Al*K*α)
CuO	0.02	0.01-0.04	0.01	metallic Cu (Cu*K*α)
SiO_2	39.73	38.70-40.21	0.59	diopside (Si*K*α)
As_2O_5	6.87	6.10-7.79	0.61	synthetic AsGa (As*L*α)
V_2O_5**	1.43	1.35-1.61	0.11	vanadinite (V*K*α)
SO_3	0.01	0.01-0.02	0.01	sphalerite (S*K*α)
F	0.04	0.00-0.19	0.00	fluorite (F*K*α)
H_2O*	2.20	2.12-2.24		
O = F	-0.02	0.08-0.00		
Total	97.44	96.85-98.26		

Notes: * H_2O calculated in order to have 2(OH) p.f.u.; **total V is reported as V_2O_5 but tetrahedral V^{5+} is calculated as 6 – (Si + As), and excess V is assigned to the octahedral sites as V^{3+}, following Nagashima and Ambruster (2010a); ***Mn^{2+}/Mn^{3+} ratio calculated (Mn^{3+}/total Mn = 0.066) in order to obtain 2(OH) groups p.f.u. and V distributed as reported.

Table 1a. Chemical data for braccoite (5 analytical points)

Table 1b.

Wt %	Valletta mine, Italy (1)	Molinello mine, Italy (2)	Ködnitz Valley, Austria (3)
As_2O_5	16.91	16.07	18.35
V_2O_5	0.59	1.67	
Sb_2O_5	0.01		
SiO_2	31.45	32.38	31.91
TiO_2			0.02
Al_2O_3			0.02
FeO	-	0.17	0.56
MnO	46.88	48.34	46.02
CaO	0.27	0.75	0.75
MgO	0.39	-	0.00
PbO	0.04		
SO_3	0.03	-	
Na_2O	0.01		0.03
F	0.11		
O=F	0.05		
Total	96.59	99.38	97.66

(1) this work (average of 3 analytical points); (2) Gramaccioli et al. (1980); (3) Albrecht (1990)

Table 1b. Comparison of chemical data available for tiragalloite from other localities.

Table 2.

h	*k*	*l*	d_{obs}(Å)	d_{calc} (Å)	Int. $_{(obs)}$	Int. $_{(calc)}$	*h*	*k*	*l*	d_{obs}(Å)	d_{calc} (Å)	Int. $_{(obs)}$	Int. $_{(calc)}$
1	-1	1	4.785	4.798	8	7.8	2	-2	2	2.393	2.399	9	2.3
0	2	0	4.723	4.710	8	10.2	0	4	-1	2.388	2.388	22	6.1
2	-2	-1	3.850	3.842	7	6.1	**4**	**-1**	**-1**	**2.381**	**2.378**	**58**	**18.7**
2	-1	-2	3.836	3.820	21	7.6	0	4	0	2.361	2.355	11	2.9
1	1	1	3.785	3.767	7	6.5	2	2	1	2.283	2.271	12	14.8
0	2	1	3.763	3.741	16	14.7	**2**	**1**	**4**	**2.226**	**2.224**	**25**	**13.6**
2	-2	0	3.741	3.748	9	7.3	0	4	-2	2.218	2.223	20	11.3
2	1	-2	3.522	3.516	8	1.6	3	-4	-1	2.204	2.202	21	24.8
0	1	2	3.438	3.420	10	1.1	1	0	4	2.186	2.181	6	4.1
1	2	-2	3.337	3.341	19	10.0	2	-3	-3	2.185	2.172	8	4.5
1	-3	0	3.310	3.308	8	8.1	3	4	-2	2.091	2.084	9	5.5
1	-2	-2	3.212	3.192	9	3.5	1	2	-4	2.082	2.084	10	14.1
1	-1	2	3.143	3.147	19	27.2	3	1	1	2.067	2.060	12	13.9
1	-3	-1	3.055	3.042	6	2.4	5	-1	-4	1.779	1.773	7	6.5
2	**-2**	**1**	**3.055**	**3.064**	**69**	**55.4**	3	1	2	1.738	1.732	7	7.0
1	-3	1	3.054	3.063	17	18.2	1	2	-5	1.693	1.694	9	5.5
1	**0**	**2**	**3.042**	**3.037**	**43**	**15.2**	4	-5	0	1.680	1.683	24	15.3
3	**-2**	**-1**	**3.012**	**3.010**	**65**	**26.9**	**4**	**3**	**-3**	**1.680**	**1.676**	**36**	**25.9**
2	-3	0	2.998	3.002	6	4.7	4	-2	-5	1.655	1.648	14	14.7
2	**-3**	**-1**	**2.985**	**2.979**	**55**	**31.5**	3	-3	3	1.595	1.599	7	5.7
1	0	-3	2.974	2.967	8	4.7	0	5	2	1.595	1.586	13	13.7
2	**1**	**-3**	**2.825**	**2.822**	**100**	**100.0**	4	0	2	1.545	1.542	7	6.1
2	**2**	**0**	**2.708**	**2.696**	**92**	**72.7**	0	3	-5	1.537	1.540	6	5.1
1	1	2	2.699	2.687	6	10.0	5	-3	-5	1.495	1.488	9	7.8
1	3	0	2.673	2.661	20	10.8	3	-1	-6	1.485	1.480	7	2.9
3	0	-3	2.655	2.647	12	17.8	6	0	-5	1.440	1.436	6	2.4
2	**-3**	**-2**	**2.627**	**2.614**	**43**	**29.4**	1	0	5	1.434	1.431	15	13.2
0	1	3	2.433	2.422	15	18.1	6	-3	0	1.434	1.434	15	12.7

Notes: *Only reflections with $I_{rel} > 6\sigma(I_{rel})$ are listed; differences in observed and calculated intensities are related to preferred orientation

Table 2. Observed and calculated X-ray powder diffraction data for braccoite. The ten strongest reflections are reported in bold *

Table 3.

Crystal system	Triclinic
Space group	$P\bar{1}$
Unit–cell dimensions	
a (Å)	9.7354(4)
b (Å)	9.9572(3)
c (Å)	9.0657(3)
α (°)	92.691(2)
β (°)	117.057(4)
γ (°)	105.323(3)
V (Å^3)	740.37(4)
Z	2
μ (mm^{-1})	5.62
F(000)	758.78
D_{calc} (g cm^{-3})	3.56
Crystal size (mm)	0.20 × 0.15 × 0.17
Radiation type	Mo$K\alpha$ (0.71073 Å)
θ–range for data collection (º)	3.5-32.3
R_{int} (%)	3.13
Reflections collected	18039
Independent reflections	4911
F_o>4σ(F)	4389
Refinement method	least-squares matrix: full
No. of refined parameters	300
Final R_{obs} (%) all data	4.14
R_1 (%) F_o>4σ(F)	3.47
wR_2 (%) F_o>4σ(F)	8.61
Highest peak/deepest hole (e$^-$ Å^{-3})	+0.81 / -0.66
Goodness of fit on F^2	1.191

Table 3. Crystal data and summary of parameters describing data collection and refinement for braccoite

Table 4.

	Site occupancy	*x/a*	*y/b*	*z/c*	U_{iso}
Na(1)	1 Na^{+}	½	0	½	0.0300(5)
Na(2)	0.521(6) Na^{+}	0.1912(3)	0.5340(2)	0.4432(3)	0.0151(7)
Mn(1)	0.953(5) Mn^{2+} 0.047(5) Mg^{2+}	0.74388(5)	0.97982(5)	0.29542(6)	0.01168(14)
Mn(2)	0.917(5) Mn^{2+} 0.083(5) Mg^{2+}	0.99723(5)	0.21282(5)	0.22004(6)	0.01045(15)
Mn(3)	0.843(5) Mn^{2+} 0.157(5) Mg^{2+}	0.86298(5)	0.88807(5)	0.02950(6)	0.00981(16)
Mn(4)	0.944(5) Mn^{2+} 0.056(5) Mg^{2+}	0.57398(5)	0.66844(4)	0.09774(5)	0.00999(15)
Mn(5)	0.953(5) Mn^{2+} 0.047(5) Mg^{2+}	0.71912(5)	0.55370(5)	0.85346(6)	0.01242(15)
T(1)	1 Si^{4+}	0.87449(9)	0.27556(8)	0.82439(10)	0.00920(15)
T(2)	1 Si^{4+}	0.03102(9)	0.23894(8)	0.60955(9)	0.00861(15)
T(3)	1 Si^{4+}	0.20746(9)	0.54939(8)	0.77372(10)	0.00943(15)
T(4)	1 Si^{4+}	0.47814(9)	0.75745(8)	0.73037(9)	0.00925(15)
T(5)	1 Si^{4+}	0.61959(9)	0.07757(8)	0.89560(9)	0.00829(15)
T(6)	0.465(3) Si^{4+} 0.535(3) As	0.60697(5)	0.71401(4)	0.48355(5)	0.00903(12)
O(1)	1 O	0.7048(2)	0.1654(2)	0.7947(3)	0.0132(4)
O(2)	1 O	0.8853(2)	0.2267(2)	0.6567(3)	0.0145(4)
O(3)	1 O	0.1110(2)	0.4094(2)	0.6204(3)	0.0133(4)
O(4)	1 O	0.3022(2)	0.6692(2)	0.7062(3)	0.0124(4)
O(5)	1 O	0.4987(2)	0.9265(2)	0.7529(3)	0.0128(4)
O(6)	1 O	0.4645(2)	0.7114(2)	0.5465(3)	0.0142(4)
O(7)	1 O	0.8556(3)	0.4331(2)	0.8222(3)	0.0144(4)
O(8)	1 O	0.9645(2)	0.7248(2)	0.0081(3)	0.0118(4)
O(9)	1 O	0.9535(2)	0.1532(2)	0.4220(2)	0.0123(4)
O(10)	1 O	0.8287(2)	0.8130(2)	0.2469(2)	0.0110(4)
O(11)	1 O	0.0805(2)	0.6058(2)	0.8035(3)	0.0143(4)
O(12)	1 O	0.6649(2)	0.4918(2)	0.0594(2)	0.0114(4)
O(13)	1 O	0.3746(2)	0.2765(2)	0.1181(2)	0.0113(4)
O(14)	1 O	0.4961(2)	0.1480(2)	0.9102(3)	0.0127(4)
O(15)	1 O	0.2404(2)	0.9490(2)	0.9367(2)	0.0112(4)
O(16)	1 O	0.6809(3)	0.8807(2)	0.4750(3)	0.0148(4)
O(17)	1 O	0.5172(2)	0.6042(2)	0.2977(3)	0.0137(4)
O(18)	1 O	0.2568(3)	0.3469(2)	0.3699(3)	0.0149(4)
O(19)	1 O	0.0897(2)	0.0502(2)	0.1728(3)	0.0134(4)
H(7)	1 H	0.937(5)	0.493(4)	0.820(5)	0.017***
H(19)**	1 H	0.179(3)	0.050(4)	0.276(3)	0.016***

Notes: *The temperature factor has the form exp(-T) where $T = 8(\pi^2)U(\sin(\theta)/\lambda)^2$ for isotropic atoms. **Atom coordinates refined with a soft constraint to O-H of 0.98 Å, ***U_{iso} refined constrained to be 1.2 the isotropic equivalent of the oxygen atom of the hydroxyl group

Table 4. Multiplicities, fractional atom coordinates, and equivalent isotropic displacement parameters ($Å^2$) for braccoite*

Table 5.

	U_{11}	U_{22}	U_{33}	U_{12}	U_{13}	U_{23}
Na(1)	0.0487(13)	0.0380(12)	0.0215(10)	0.0280(10)	0.0230(10)	0.0175(9)
Na(2)	0.0233(13)	0.0130(12)	0.0087(11)	0.0032(9)	0.0090(10)	0.0023(8)
Mn(1)	0.0098(2)	0.0107(2)	0.0128(2)	0.00149(16)	0.00516(17)	0.00090(16)
Mn(2)	0.0103(2)	0.0107(2)	0.0104(2)	0.00265(16)	0.00545(17)	0.00342(16)
Mn(3)	0.0098(2)	0.0093(2)	0.0112(2)	0.00304(17)	0.00566(18)	0.00310(16)
Mn(4)	0.0093(2)	0.0091(2)	0.0111(2)	0.00244(16)	0.00485(17)	0.00261(15)
Mn(5)	0.0125(2)	0.0113(2)	0.0153(2)	0.00397(17)	0.00813(18)	0.00284(16)
T(1)	0.0087(3)	0.0102(3)	0.0101(3)	0.0031(3)	0.0055(3)	0.0040(3)
T(2)	0.0085(3)	0.0092(3)	0.0079(3)	0.0025(3)	0.0039(3)	0.0027(3)
T(3)	0.0086(3)	0.0088(3)	0.0110(3)	0.0021(3)	0.0050(3)	0.0039(3)
T(4)	0.0097(3)	0.0090(3)	0.0093(3)	0.0025(3)	0.0049(3)	0.0038(3)
T(5)	0.0081(3)	0.0091(3)	0.0086(3)	0.0029(3)	0.0044(3)	0.0038(3)
T(6)	0.0098(2)	0.00979(19)	0.00859(19)	0.00275(14)	0.00542(15)	0.00280(13)
O(1)	0.0107(9)	0.0153(9)	0.0142(9)	0.0024(7)	0.0072(8)	0.0071(8)
O(2)	0.0118(9)	0.0220(10)	0.0113(9)	0.0053(8)	0.0069(8)	0.0043(8)
O(3)	0.0159(10)	0.0102(9)	0.0104(9)	0.0016(7)	0.0049(8)	0.0020(7)
O(4)	0.0112(9)	0.0131(9)	0.0129(9)	0.0020(7)	0.0065(7)	0.0052(7)
O(5)	0.0138(9)	0.0087(8)	0.0121(9)	0.0012(7)	0.0045(8)	0.0036(7)
O(6)	0.0129(9)	0.0199(10)	0.0099(9)	0.0037(8)	0.0064(8)	0.0032(8)
O(7)	0.0134(10)	0.0108(9)	0.0214(11)	0.0042(8)	0.0101(8)	0.0058(8)
O(8)	0.0112(9)	0.0132(9)	0.0112(9)	0.0056(7)	0.0046(7)	0.0034(7)
O(9)	0.0137(9)	0.0134(9)	0.0087(9)	0.0022(7)	0.0056(7)	0.0019(7)
O(10)	0.0107(9)	0.0121(9)	0.0091(9)	0.0040(7)	0.0036(7)	0.0023(7)
O(11)	0.0148(10)	0.0140(9)	0.0200(10)	0.0063(8)	0.0120(8)	0.0069(8)
O(12)	0.0115(9)	0.0114(9)	0.0103(9)	0.0035(7)	0.0044(7)	0.0038(7)
O(13)	0.0128(9)	0.0120(9)	0.0103(9)	0.0051(7)	0.0059(7)	0.0040(7)
O(14)	0.0128(9)	0.0140(9)	0.0142(9)	0.0062(7)	0.0078(8)	0.0047(7)
O(15)	0.0115(9)	0.0110(9)	0.0104(9)	0.0034(7)	0.0048(7)	0.0044(7)
O(16)	0.0175(10)	0.0130(9)	0.0136(10)	0.0031(8)	0.0081(8)	0.0048(8)
O(17)	0.0142(9)	0.0142(9)	0.0105(9)	0.0017(8)	0.0060(8)	0.0003(7)
O(18)	0.0133(9)	0.0159(10)	0.0165(10)	0.0068(8)	0.0066(8)	0.0069(8)
O(19)	0.0125(9)	0.0153(9)	0.0112(9)	0.0049(8)	0.0044(8)	0.0034(7)

Notes: * The temperature factor has the form exp(-T) where $T = 2\pi^2\Sigma_{ij}(h(i)h(j)U(i,j)a^*(i)a^*(j))$.

Table 5. Anisotropic displacement parameters for braccoite (Å)*

Table 6.

Na(1)	- O(5) (×2)	2.444(2)	Mn(2)	- O(11)	2.119(2)	Mn(5)	- O(7)	2.108(2)	T(3)	- O(11)	1.604(2)	T(6)	-O(16)	1.646(2)
	- O(16) (×2)	2.451(2)		- O(9)	2.136(2)		- O(17)	2.159(2)		- O(12)	1.618(2)		-O(17)	1.667(2)
	- O(1) (×2)	2.613(2)		- O(19)	2.161(2)		- O(13)	2.178(2)		- O(4)	1.628(2)		-O(18)	1.670(2)
	- O(6) (×2)	2.877(2)		- O(15)	2.189(2)		- O(12)	2.231(2)		- O(3)	1.642(2)		-O(6)	1.719(2)
<Na(1)	- O>	2.596		- O(18)	2.222(2)		- O(8)	2.270(2)	<T(3)	- O>	1.623	<T(6)	- O>	1.675
	$^{**}V$(Å^3)	26.007		- O(8)	2.346(2)		- O(18)	2.374(2)		V(Å^3)	2.188		V(Å^3)	2.403
			<Mn(2)	- O>	2.196	<Mn(5)	- O>	2.220		σ^2*	7.846		σ^2*	12.945
Na(2)	- O(18)	2.285(3)		V(Å^3)	13.711		V(Å^3)	14.066		λ*	1.0019		λ*	1.0032
	- O(4)	2.292(3)		σ^2*	67.545		σ^2*	86.772						
	- O(7)	2.293(3)		λ*	1.0207		λ*	1.0260	T(4)	- O(13)	1.602(2)			
	- O(3)	2.355(3)								- O(4)	1.612(2)			
	- O(6)	2.484(3)	Mn(3)	- O(19)	2.116(2)	T(1)	- O(8)	1.613(2)		- O(5)	1.633(2)			
	- O(11)	2.513(3)		- O(8)	2.156(2)		- O(1)	1.617(2)		- O(6)	1.643(2)			
	- O(2)	2.753(3)		- O(19)	2.163(2)		- O(7)	1.626(2)	<T(4)	- O>	1.623	H(7)	-O(7)	0.86(4)
	- O(3)	2.944(3)		- O(13)	2.191(2)		- O(2)	1.632(2)		V(Å^3)	2.181	H(7)	…O(11)	1.62(4)
<Na(2)	- O>	2.490		- O(15)	2.199(2)	<T(1)	- O>	1.622		σ^2*	14.064	O(7)	…O(11)	2.48(1)
	V(Å^3)	25.210		- O(10)	2.272(2)		V(Å^3)	2.178		λ*	1.0033	O(7)-	H(7)…O(11)	176.37(2)°
			<Mn(3)	- O>	2.183		σ^2*	15.761						
Mn(1)	- O(9)	2.069(2)		V(Å^3)	13.523		λ*	1.0038	T(5)	- O(14)	1.592(2)	H(19)	-O(19)	0.95(2)
	- O(10)	2.150(2)		σ^2*	55.177					- O(15)	1.607(2)	H(19)	…O(16)	1.99(2)
	- O(16)	2.177(2)		λ*	1.0174	T(2)	- O(9)	1.596(2)		- O(1)	1.634(2)	O(19)	…O(16)	2.855(10)
	- O(14)	2.190(2)					- O(10)	1.626(2)		- O(5)	1.679(2)	O(19)-	H(19)…O(16)	150.34(18)°
	- O(15)	2.308(2)	Mn(4)	- O(14)	2.107(2)		- O(2)	1.635(2)	<T(5)	- O>	1.628			
	- O(5)	2.627(2)		- O(12)	2.190(2)		- O(3)	1.647(2)		V(Å^3)	2.183			
<Mn(1)	- O>	2.253		- O(17)	2.199(2)	<T(2)	- O>	1.626		σ^2*	41.722			
	V(Å^3)	14.087		- O(10)	2.220(2)		V(Å^3)	2.200		λ*	1.0098			
	σ^2*	170.515		- O(12)	2.246(2)		σ^2*	9.140						
	λ*	1.0617		- O(13)	2.287(2)		λ*	1.0021						
			<Mn(4)	- O>	2.208									
				V(Å^3)	13.939									
				σ^2*	67.478									
				λ*	1.0204									

Notes: *Mean quadratic elongation (λ) and the angle variance (σ^2) were computed according to Robinson *et al*. (1971); ** V = polyhedral volume

Table 6. Main interatomic distances (Å) and geometrical parameters for braccoite

Table 7.

	T(1)	T(2)	T(3)	T(4)	T(5)	T(6)	M(1)	M(2)	M(3)	M(4)	M(5)	Na(1)	Na(2)	H(7)	H(19)		+ H contrib
O(1)	1.013				0.968							0.115 ×2↓				2.096	
O(2)	0.975	0.965											0.047			1.987	
O(3)		0.937	0.949										0.116 0.030			2.032	
O(4)			0.985	1.026									0.134			2.145	
[IV]O(5)				0.972	0.863		0.120					0.169 ×2↓				2.123	
[IV]O(6)				0.946		1.029						0.063 ×2↓	0.086			2.124	
[IV]O(7)	0.988										0.409		0.133	1.019 0.475		1.531	2.550 2.006
[IV]O(8)	1.024							0.223	0.353		0.271					1.871	
O(9)		1.073					0.457	0.376								1.906	
[IV]O(10)		0.988					0.369		0.264	0.306						1.928	
[IV]O(11)			1.050					0.393					0.081	0.255 0.475		1.524	1.779 1.999
O(12)			1.010							0.331 0.287	0.298					1.927	
[IV]O(13)				1.056					0.323	0.260	0.341					1.980	
O(14)					1.084		0.332			0.410						1.826	
[IV]O(15)					1.041		0.248	0.328	0.317							1.934	
[IV]O(16)						1.240	0.344					0.166 ×2↓			0.162	1.749	1.911
O(17)						1.173				0.323	0.358					1.855	
[IV]O(18)						1.167		0.302			0.211		0.136			1.815	
O(19)								0.353	0.392 0.347						0.824	1.091	1.915
	4.000	3.963	3.994	3.999	3.956	4.609	1.870	1.975	1.996	1.917	1.888	1.026	0.763	1.274 0.950	0.986		37.38
F.C.*	4.000	4.000	4.000	4.000	4.000	4.630	2.000	2.070	2.240	2.030	2.000	1.000	0.560	1.000	1.000	37.96	

Note: anion sites coordination reported only for coordination other than 3. * F.C: = formal charge at site on the basis of chemical formula

Table 7. Bond valence calculations for braccoite (Brown, 1981)

Table 8.

Site	Refined site-scattering (e*pfu*)	Assigned site-population (*apfu*)	Calculated site-scattering (e*pfu*)	<X-φ>$_{calc.}$* (Å)	<X-φ>$_{obs.}$ (Å)	Ideal composition (*apfu*)
		Cations				
Mn(1)	24.39(7)	0.98 Mn^{2+} + 0.01 Mg + 0.01 Ca	24.82	2.191	2.253	Mn^{2+}
Mn(2)	23.93(7)	0.87 Mn^{2+} + 0.07 Mn^{3+} + 0.06 Mg	24.22	2.170	2.196	Mn^{2+}
Mn(3)	22.96(7)	0.56 Mn^{2+} + 0.32 Mn^{3+} + 0.10 Mg + 0.01 V^{3+} + 0.01 Al^{3+} +	23.53	2.130	2.183	Mn^{2+}
Mn(4)	24.28(7)	0.96 Mn^{2+} + 0.03 Mn^{3+} + 0.01 Mg	24.87	2.183	2.208	Mn^{2+}
Mn(5)	24.39(7)	0.99 Mn^{2+} + 0.01 Mg	24.87	2.189	2.220	Mn^{2+}
T(6)	24.17(6)	0.48 As + 0.37 Si + 0.15 V^{5+}	24.47	1.671	1.675	As
Na(1)	11	1.00 Na	11.00	2.560	2.596	Na**
Na(2)	5.72(6)	0.56 Na + 0.44 □	6.16	2.560	2.490	Na,□
		Anions				
$^{[IV]}$O(19)		0.98 OH + 0.02 F				OH

X = cation, φ = O, OH, F;
* calculated by summing constituent ionic radii; values from Shannon (1976);
** site in special position, half multiplicity;

Table 8. Refined site-scattering and assigned site-populations for braccoite

Table 9.

	Braccoite	Saneroite	Scheuchzerite	Steedeite
Reference	(1)	(2, 3)	(4)	(5)
Formula	$NaMn^{2+}{}_5[Si_5AsO_{17}(OH)](OH)$	$NaMn^{2+}{}_5[Si_5VO_{17}(OH)](OH)$	$NaMn^{2+}{}_9[Si_9O_{25}(OH)(VO_3)](OH)$	$NaMn_2[Si_3BO_9](OH)_2$
Crystal system	Triclinic	Triclinic	Triclinic	Triclinic
Space group	$P\bar{1}$	$P\bar{1}$	$P\bar{1}$	$P\bar{1}$
a (Å)	9.7354(4)	9.741(5)	9.831(5)	6.837(1)
b	9.9572(3)	9.974(7)	10.107(5)	7.575(2)
c	9.0657(3)	9.108(5)	13.855(7)	8.841(2)
α (°)	92.691(2)	92.70(4)	86.222(10)	99.91(3)
β	117.057(4)	117.11(4)	73.383(9)	102.19(3)
γ	105.323(3)	105.30(4)	71.987(9)	102.78(3)
V (Å^3)	740.37(4)	744.16	1254.2(10)	424.81(1)
Z	2	2	2	2
Axial ratios (*a*:*b*:*c*)	0.978:1:0.910	0.977:1:0.913	0.973:1:1.371	0.9026:1:1.1671
D_{meas} (g cm^{-3})	n.d.	3.47	3.50(2)	n.d.
D_{calc} (g cm^{-3})	3.56	3.51	3.47	3.104
Strongest lines in the powder pattern: d_{obs} (Å)(*I*)	3.774(30), 3.514(30), 3.042(60), 3.005(60), 2.973(80), 2.821(100), 2.696(90), 2.620(30), 2.676(50), 1.673(30)	3.06(s), 2.83(s), 2.70(s), 3.01(m), 2.98(m), 2.62(m), 2.20(m)	2.71(100), 3.09(80), 7.91(70),8.68(50), 2.92(40), 3.22(40), 3.94(30), 4.83(30)	8.454 (100), 7.234(39), 3.331(83), 3.081(38), 2.859(52), 2.823(80)
Optical character	biaxial (+)	biaxial (–)	biaxial (+)	biaxial
Colour	brown-red	bright orange	yellow-orange	pale pink to colourless
Pleochroism	*X* = brownish yellow, *Y* = dark yellow , *Z* = yellow	*X* = deep orange; *Y* = lemon-yellow; *Z* = yellow-orange	*X* = brown yellow; *Y* = pale yellow	Not observed
Hardness (Mohs)	n.d.	n.d.	2-3	n.d.
Streak	pale-yellow	white	yellow-orange	white
Luster	vitreous to resinous	resinous to greasy	vitreous	vitreous
Habit and forms	subhedral	tabular-prismatic crystals	acicular and prismatic crystals	acicular crystals
Association	aegirine, hematite, tiragalloite, quartz, unidentified Mn oxides, and Mn silicates	quartz, baryte, caryopilite, ganophyllite, medaite, palenzonaite, pyrobelonite, fianelite, parsettensite, rhodochrosite, kutnahorite, aegirine	saneroite, tiragalloite	aegirine, analcime, catapleiite, eudialyte, microcline nepheline, natrolite, pyrrhotite, sérandite, sodalite, thermonatrite

Refs: (1) this work; (2) Lucchetti *et al.* (1981); (3) Nagashima and Armbruster (2010a); (4) Brugger *et al.* (2006); (5) Haring and McDonald (2014).

Table 8. Comparison of minerals related to braccoite. References are given in brackets

Table 9.

	Saneroite (Molinello mine, Italy)[1]				Saneroite (Fianel, Switzerland)[1]		Braccoite (Valletta mine, Italy)[2]	
	specimen 1		specimen 2					
	Wt%	SD	Wt%	SD	Wt%	SD	Wt%	SD
SiO_2	39.99	1.06	39.06	0.65	41.03	0.98	39.73	0.59
Al_2O_3	0.02	0	0.01	0.02	0.01	0.02	0.04	0.04
MnO	42.2	1.38	40.33	1.06	41.53	1.12	39.00	0.41
Mn_2O_3	-	-	-	-	-	-	3.07	0.53
MgO	0.01	0.02	0.00	0.00	0.03	0.04	0.96	0.05
CaO	0.13	0.05	0.11	0.04	0.33	0.12	0.05	0.01
Na_2O	4.34	0.28	4.36	0.27	4.52	0.25	4.06	0.2
K_2O	0	0.01	0.01	0.01	0.01	0.01	-	-
CuO	0.1	0.14	0.2	0.24	0.14	0.2	0.02	0.01
NiO	0.03	0.04	0.03	0.03	0.02	0.03	-	-
V_2O_5	7.15	1.8	7.78	0.7	6.05	1.23	1.43	0.11
As_2O_5	1.22	1.27	1.92	1.65	1.31	1.85	6.87	0.61
SO_3	-	-	-	-	-	-	0.01	0.01
F	-	-	-	-	-	-	0.04	0
Total	95.19		93.81		94.98		95.28	

Refs: (1) Nagashima and Armbruster, 2010a; (2) this work

Table 9. Comparison of chemical data between saneroite from Molinello mine (Italy) and Fianel (Switzerland) and braccoite from Valleta (this work).

FIGURE CAPTIONS

Figure 1. a) Picture of the rocks containing braccoite; b) Picture of rare red crystalline masses with brown hue of braccoite holotype intergrown with orange tiragalloite forming a thin layer on hematite and quartz (FoV: 5 mm). Photo of R. Bracco.

Figure 2. BSE image of a section of a quartz (qtz) vein showing braccoite (brac) and tiragalloite (tirag) used during the WDS analyses. Small spot within quartz is baryte (bary)

Figure 3. Raman spectra of braccoite in the 200-4000 cm^{-1} region and between 200 and 1200 cm^{-1}.

Figure 4. Raman spectra of tiragalloite in the 150-4000 cm^{-1} region and between 150 and 1200 cm^{-1}.

Figure 5. Detail of the braccoite structure showing the bands of Mn octahedra and the silicate chains. Blue: Si tetrahedra; green: As-Si tetrahedron; yellow: Mn octahedra; light blue: Na.; white: H. Violet double arrow shows the short *Na*(2)…*H*(7) distance. Approx. vector of projection is [5$\bar{1}$5]. Design obtained with Vesta 3 (Momma and Izumi, 2011).

Figure 1a.

Figure 1b.

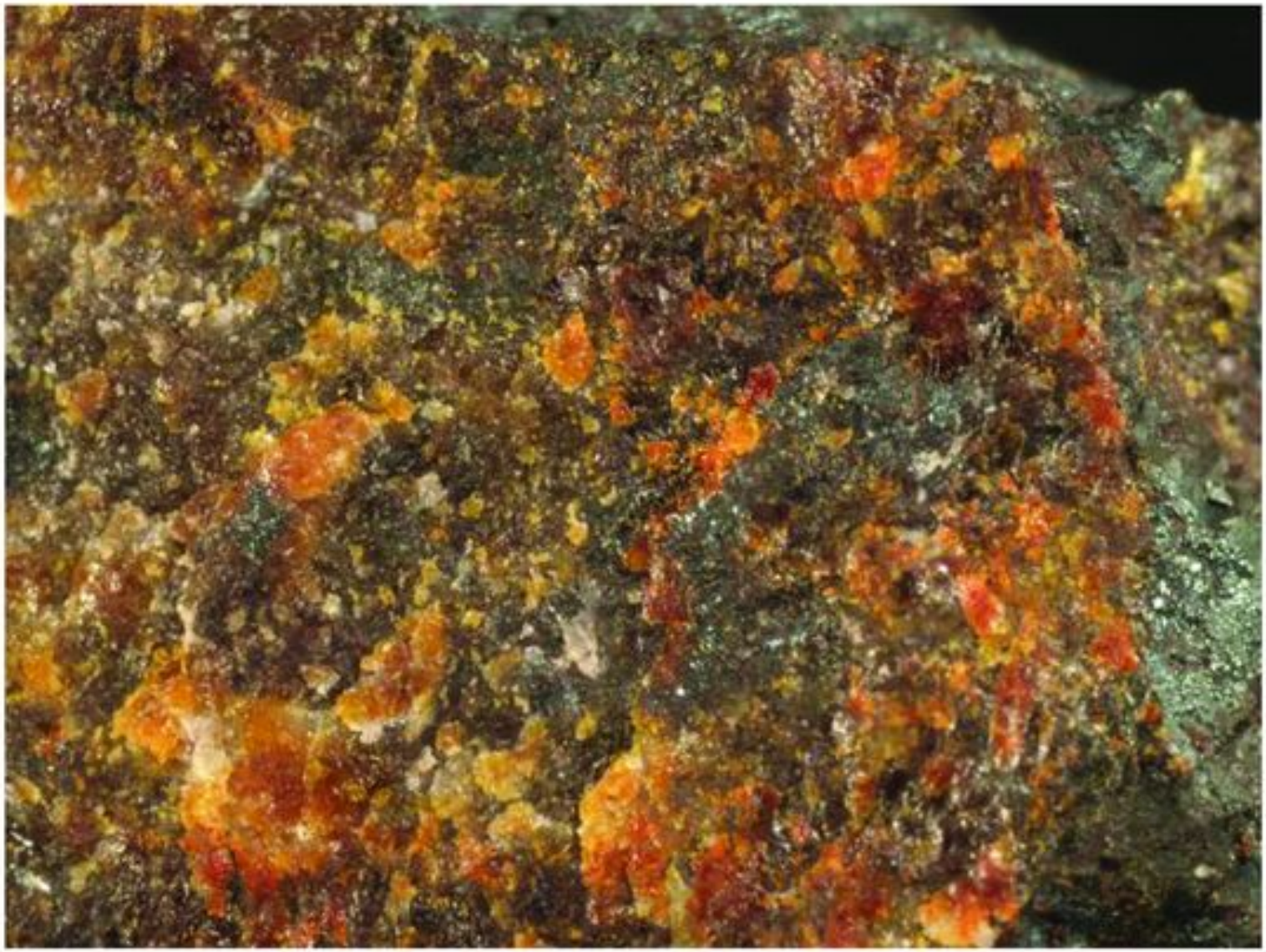

Figure 2.

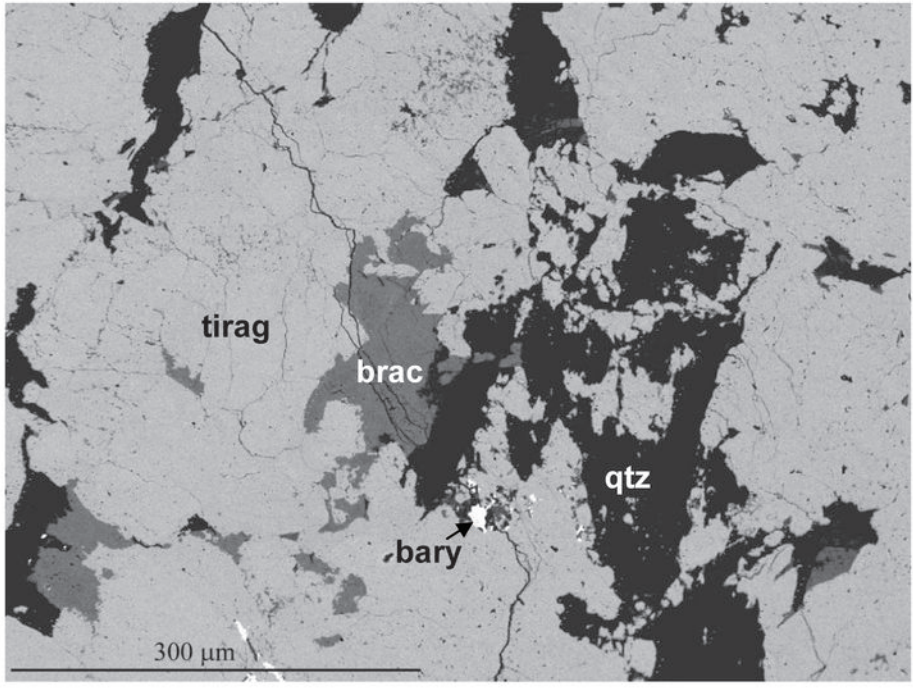

Figure 3.

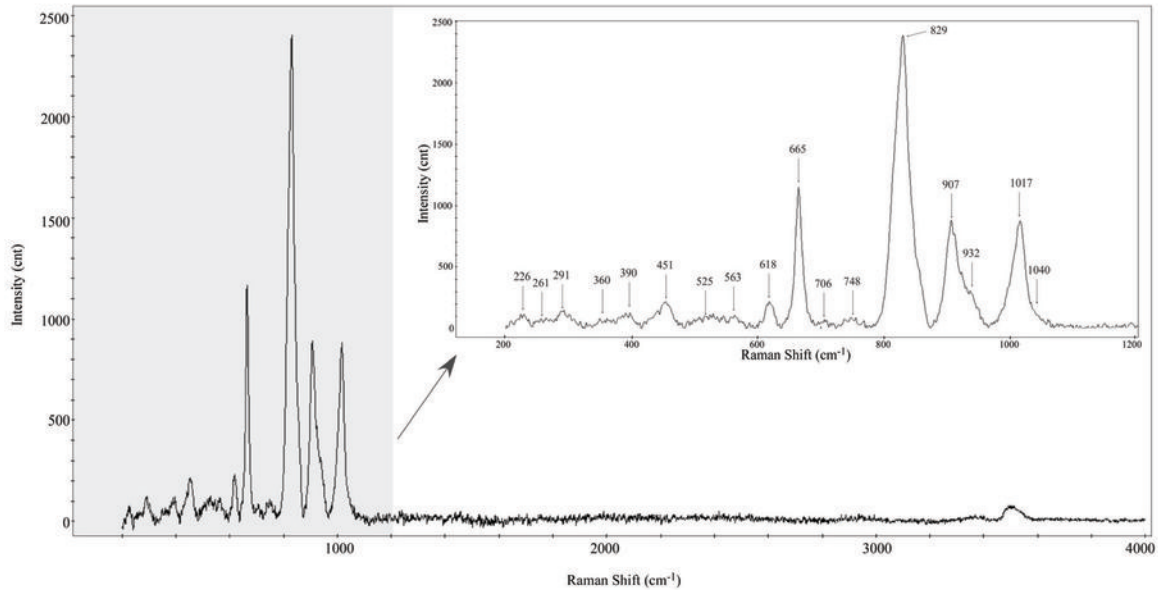
Intensity (cnt)
Raman Shift (cm-1)
226
261
291
360
390
451
525
563
618
665
706
748
829
907
932
1017
1040

Figure 4.

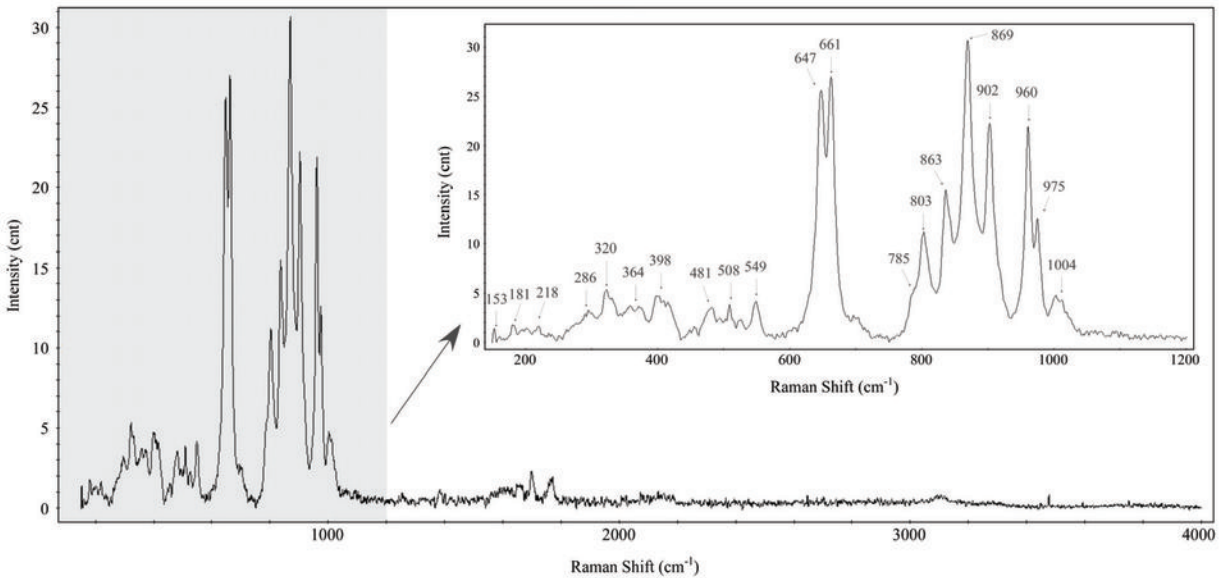
Intensity (cnt)
Raman Shift (cm-1)
153
181
218
286
320
364
398
481
508
549
647
661
785
803
863
869
902
960
975
1004

Figure 5.

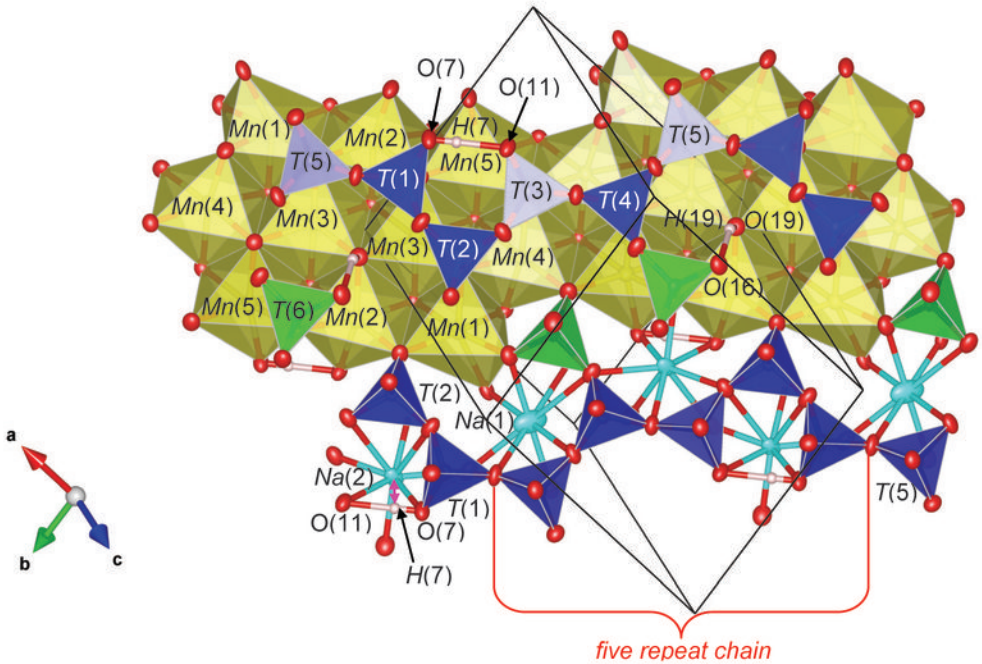
O(7)
O(11)
H(7)
Mn(1)
Mn(2)
T(5)
T(1)
Mn(5)
T(3)
T(4)
T(5)
Mn(4)
Mn(3)
H(19)
O(19)
Mn(3)
T(2)
Mn(4)
O(16)
Mn(5)
T(6)
Mn(2)
Mn(1)
T(2)
Na(1)
Na(2)
T(1)
T(5)
O(11)
O(7)
H(7)
a
b
c
five repeat chain